# Microconfined flow behavior of red blood cells by image analysis techniques

Giovanna TOMAIUOLO[1,2*], Luca LANOTTE[1,3], Antonio CASSINESE[4], Stefano GUIDO[1,2]

* Corresponding author: Tel.: ++39 081 7682261; Fax: ++39 081 2391800; Email: g.tomaiuolo@unina.it
1 Dipartimento di Ingegneria Chimica, dei Materiali e della Produzione Industriale, Università di Napoli Federico II, Italy
2 CEINGE Biotecnologie avanzate, Napoli, Italy
3 Univ. Grenoble 1/CNRS, LIPhy UMR 5588, BP 87, 38041 Grenoble, France
4 CNR-SPIN and Dipartimento di Scienza Fisiche, Università di Napoli Federico II, Italy

**Abstract** Red blood cells (RBCs) perform essential functions in human body, such as gas exchange between blood and tissues, thanks to their ability to deform and flow in the microvascular network. The high RBC deformability is mainly due to the viscoelastic properties of the cell membrane. Since an impaired RBC deformability could be found in some diseases, such as malaria, sickle cell anemia, diabetes and hereditary disorders, there is the need to provide further insight into measurement of RBC deformability in a physiologically-relevant flow field. Here, we report on an imaging-based *in vitro* systematic microfluidic investigation of RBCs flowing either in microcapillaries or in a microcirculation-mimicking device containing a network of microchannels of diameter comparable to cell size. RBC membrane shear elastic modulus and surface viscosity have been investigated by using diverging channels, while RBC time recovery constant have been measured in start-up experiments. Moreover, RBC volume and surface area have been measured in microcapillary flow. The comprehension of the single cell behavior led to the analysis of the RBC flow-induced clustering. Overall, our results provide a novel technique to estimate RBC deformability, that can be used for the analysis of pathological RBCs, for which reliable quantitative methods are still lacking.

**Keywords:** Red blood cells, Deformability, Clustering, Microcirculation

## 1. Introduction

In microcirculation *in vivo*, red blood cells (RBCs) travel through microvessels with diameter smaller than cell size in order to allow optimal gas transfer between blood and tissues (Wang and Popel, 1993). In such microconfined conditions RBC shape departs from the classical biconcave geometry at rest by taking deformed configurations, resembling a bullet or a parachute, depending on flow rate and microvessel diameter (Guido and Tomaiuolo, 2009; McHedlishvili and Maeda, 2001; Wang and Popel, 1993). The high RBC deformability is mainly due to the viscoelastic properties of the cell membrane, especially shear modulus and surface viscosity(Guido and Tomaiuolo, 2009). Pathological alterations of RBC deformability are known to be implicated in several diseases, including diabetes, malaria, and sickle cell disease (Barabino et al., 2010; Buys et al., 2013; Hosseini and Feng, 2012; Shattil et al., 2000). In light of such pathophysiological relevance, the measurement of RBC deformability has been the subject of a number of studies from single cell analysis (micropipette aspiration (Engstrom and Meiselman, 1995; Evans, 1973; Hochmuth, 2000) and optical tweezers (Hénon et al., 1999; Mills et al., 2007; Zhang and Liu, 2008)) to flow techniques (ektacytometry (Bessis et al., 1980). Recently, microfluidic techniques (Whitesides, 2006), that are suitable to testing a large number of cells in a physiologically relevant flow field, have been applied to design flow geometries resembling the microvascular network (Abkarian et al., 2008; Shevkoplyas et al., 2003; Tomaiuolo et al., 2011; Tsukada et al., 2001). In this work, we report on an imaging-based *in vitro*

systematic fluid dynamic investigation of RBC suspensions flowing either in microcapillaries or in a microcirculation-mimicking device containing a network of microchannels of diameter comparable to cell size. RBC membrane rheological behavior is investigated by analyzing the transient behavior of RBC shape in confined flow and by measuring the membrane viscoelastic properties in converging/diverging microchannels. RBC geometrical parameters, such as RBC volume, surface area, and distribution width (RDW), which is a measurement of the size variation and can be used as a significant diagnostic and prognostic tool in cardiovascular and thrombotic disorders (Montagnana et al., 2012), have been measured in microcapillary flow using high-speed microscopy. The obtained results provide a novel microfluidics methodology to measure RBC biomechanical properties, which are potential diagnostic parameters of altered cell deformability The comprehension of the single cell behavior led to the analysis of the RBC flow-induced clustering.

In order to study the effect of reduced deformability of the RBC membrane, the flow behavior of glutaraldehyde (GA)-hardened RBCs has been analyzed, being GA a crosslinking agent of the proteins of the RBC membrane, able to change the viscoelastic properties of RBC membrane.

## 2. Materials and Methods

### 2.1 Blood samples

Fresh venous blood samples, drawn from healthy donors and used within 4 h from collection, are centrifuged to separate RBCs from white cells and platelets. Then the RBCs are re-suspended in plasma and diluted with ACD anticoagulant and human albumin to a concentration of 1% for single cell experiments, or 10% by volume for clustering tests.

### 2.2 Experimental apparatus

Images of the flowing RBCs are acquired by a high speed video camera (operated up to 1000 frames/s) and by using a high magnification oil immersion objective (100x). The experiments are carried out either in 6.6 or 10 μm diameter silica microcapillaries placed in a flow cell (Figure 1a) and in a microfluidic device (Figure 1b).

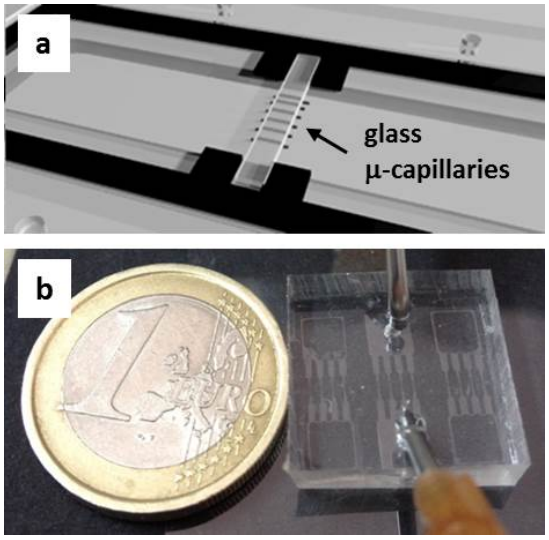


**Figure 1:** a) detail of the flow cell with the 6.6 and 10 μm glass microcapillaries; b) PDMS microfluidic device.

The latter is made of PDMS and is fabricated by using soft-lithography techniques with SU-8 as photoresist. The network pattern consists of a network of bifurcating channels of decreasing width (down to 10 μm), including converging–diverging flow sections, to mimic human microcirculation network.

## 3. Results

### 3.1 Single RBC velocity and shape

The observed RBC shape is shown in Figure 2 as a function of cell velocity. In a microcapillary of diameter D=6.6 μm all RBCs showed the typical axisymmetric parachute-like shape, tending to an asymptotic configuration at increasing cell velocity (Tomaiuolo et al., 2009). Asymmetric shapes are mostly observed (together with axisymmetric ones in an almost 1: 1 ratio) in the 10 μm microcapillary, where the flow is still confined, causing RBC deformation, as shown in Figure 3. Up to RBC velocity around 1 mm $s^{-1}$ asymmetry was apparently the result of folding of the cell membrane.

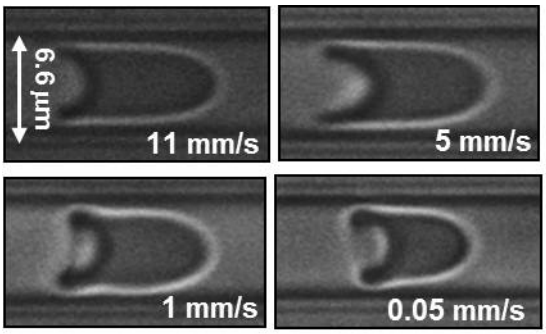


**Figure 2:** Images of RBCs flowing in a 6.6 μm microcapillary at different velocities.

At higher RBC velocities asymmetric shapes were due to out-of-axis cell position (which is prevented in the smallest microcapillary by the effect of confinement) and were associated with a slightly lower cell velocity.

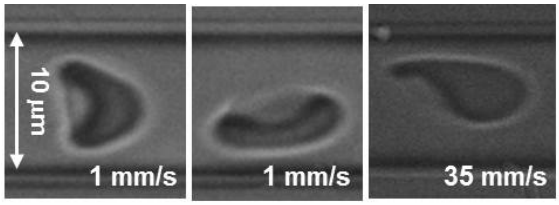


**Figure 3:** Images of RBCs flowing in a 10 μm microcapillary at different velocities.

A quantitative analysis of RBC shape is presented in Figure 4a, where cell deformation index (measured as the ratio between the long side and the short side of a bounding box enclosing the cell body) is plotted as a function of RBC velocity for D = 6.6 μm. An increasing trend is observed, with a leveling-off of cell length with increasing RBC velocity. These results provide quantitative evidence of the asymptotic shape which can be observed in the images of Figure 2.
The continuous line represents prediction of the model by Secomb et al. for D=6 μm (Secomb et al., 1986). In the theoretical model, calculations are based on the data of elastic shear modulus and bending rigidity of the membrane from the literature (Guido and Tomaiuolo, 2009) and on the classical average values of surface area (135 $\mu m^2$) and volume (90 $\mu m^3$) for healthy RBCs. The suspending fluid viscosity is taken equal to be 1 cP, close to the experimental value. The fact that there are no adjustable parameters in model calculations makes more remarkable the good agreement with the experimental data. In Figure 4b the change in minimum apparent plasma-layer thickness is shown as a function of cell velocity for D=6.6 μm. The minimum apparent plasma-layer thickness, defined as (D-d)/2, where D is the capillary diameter and d is the cell diameter (as shown in the inset of Figure 4b), is about 1.3 μm for the D= 6.6 μm. There is an initial increasing trend (between 0 and 4 mm/sec) where the cells are undergoing shape changes, followed by a plateau (for velocities greater than 4 mm/sec), where any additional deformation occurs. The evaluation of plasma-layer thickness is a novel analysis which confirms the existence of RBC asymptotic shape at high flow velocities.

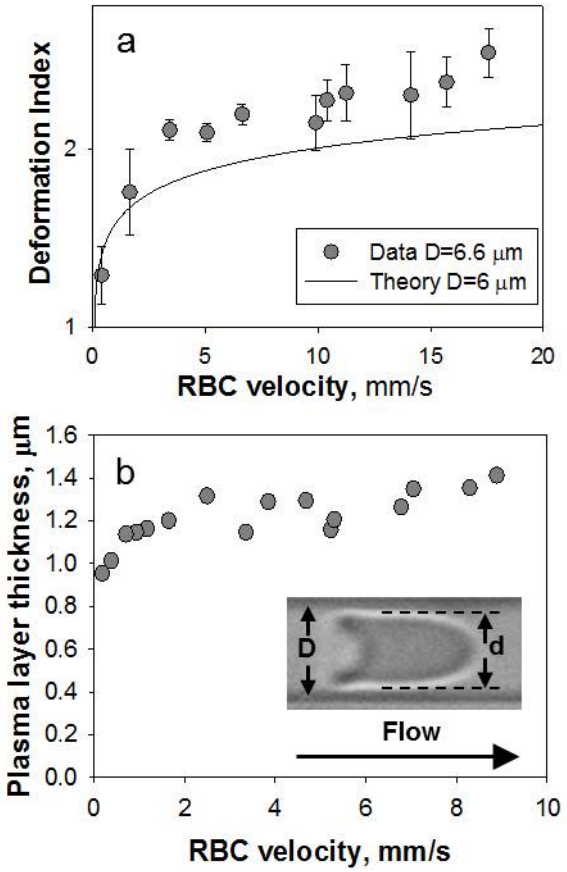


**Figure 4:** a) Plot of RBC deformation index as a function of cell velocity at D = 6.6 μm, the solid lines being theoretical predictions (Secomb, 1987; Secomb et al., 1986); b) Plot of plasma-layer thickness as a function of RBC velocity at D= 6.6 μm. In the inset the dimensions used to define the plasma-layer are shown.

### 3.2 RBC start-up shape dynamics

In order to evaluate RBC relaxation time

constant, RBC shape dynamics during start-up of shear flow has been observed (Tomaiuolo and Guido, 2011). Experiments were carried out in microcapillaries with inner diameter of 10 μm, the shape observation starting from the biconcave shape at rest to reaching the asymptotic steady state configuration. The effect of glutaraldehyde (GA), at different concentrations on RBC deformability was also investigated, as a model of cellular membrane disorders in which RBC deformability is impaired, such as diabetes (Cecchin et al., 1987), hereditary membrane disorders (include spherocytosis, elliptocytosis, ovalocytosis and stomatocytosis) (Da Costa et al., 2013; Kohno et al., 1997), hypercholesterolemia (Kohno et al., 1997), paroxysmal nocturnal hemoglobinuria (Smith, 1985), malaria (Hosseini and Feng, 2012), sickle cell anemia (Barabino et al., 2010), etc.

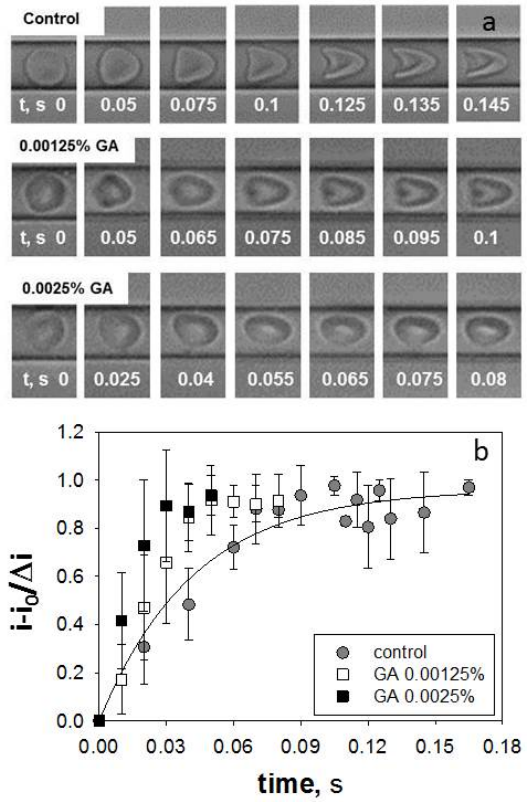


**Figure 5:** a) Images at high magnification (100x) of RBC transient shape at start-up for control and glutaraldehyde hardened RBCs at the same experimental conditions (i.e. ΔP/L=4 mm Hg/mm, corresponding to cell velocity of about 0.1 cm/s). Flow is from left to right; b) Quantitative analysis of RBC shape evolution as a function of time up for control and glutaraldehyde hardened RBCs.

Typical examples of shape evolution are shown in Figure 5a, where time 0 corresponds to the onset of cell motion. Quantitative measurements of cell shape during start-up were obtained by image analysis based on the comparison between the mean intensity (expressed by the mean gray level) of the cell body at rest ($i_0$) and during the start-up flow (i). The difference $i-i_0$ was made dimensionless by the maximum difference of intensity $\Delta i$ in the recorded sequence. In Figure 5b the dimensionless ratio $(i-i0)/\Delta i$ is plotted as a function of time, for normal RBCs (control) and GA hardened RBCs.Regarding control sample, an increasing trend, with a leveling off corresponding to ca. 0.1 s is shown. Indeed, the time dependence of the ratio $i-i_0/\Delta i$ can be taken as representative of the time evolution of the RBC shape during start-up flow, since the intensity difference approaches a constant plateau value when the cell reaches a steady state shape. This value is independent on the imposed flow rate and thus corresponds to an intrinsic property of the cell membrane. Moreover, it is in good agreement with the results from the literature (Guido and Tomaiuolo, 2009; Hochmuth et al., 1979; Waugh and Evans, 1979). RBCs hardened by glutaraldehyde present lower values of the time constant, the plateau starting at time lower than 0.1 s, as shown in Figure 5b. Thus, the importance and the novelty of this technique is that it can be used to discriminate between RBCs with different membrane rheological parameters, fundamental for the study of pathological blood samples.

### 3.3 RBC membrane viscoelasticity

A PDMS microfluidic device, as described in the methods section, has been used to measure the viscosity and the elastic shear modulus of RBC membrane(Tomaiuolo et al., 2011). In particular, RBCs flow in a diverging channel region, as shown in Fig. 6 was investigated. The RBC deformation index DI, measured as the ratio between the long side and the short side of a bounding box enclosing the cell body, has been plotted as a function of the z coordinate at two values of pressure drops in Figure 6. It can be seen that DI is a decreasing function of

z, due to the more rounded shapes as RBCs approach the divergent end.

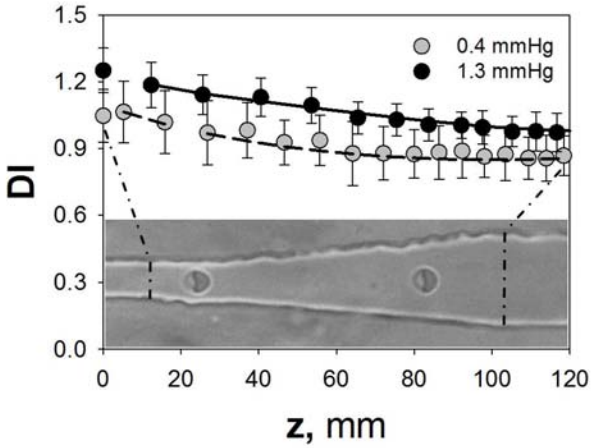


**Figure 6:** The deformation index vs z in the divergent channel region at two pressure drops. Lines are obtained by best-fitting the Kelvin–Voigt model.

The fluid dynamic action on a cell travelling along the centerline of the divergent channel was described as a uniaxial compressional stress, and the cell shape change can be described by using the Kelvin–Voigt model (Hochmuth et al., 1979), which is based on the parallel combination of a spring and a dashpot. The two elements are associated with the elastic and the viscous response of the cell membrane, respectively. A best fitting procedure was applied to both datasets of Figure 6, obtaining the value of 0.006 dyn $cm^{-1}$ for μ (shear modulus) and of 0.055 cP·cm for η (surface viscosity). These values are in good agreement with experimental results from the literature (0.006–0.009 for μ, and 0.047–0.1 for η) (Guido and Tomaiuolo, 2009).

### 3.4 RBC Area and Volume

The microfluidic approach was also used to measure, simultaneously, the surface area and the volume of RBCs flowing in microcapillaries (Tomaiuolo et al., 2012b). Surface area measurements can be used as diagnostic parameters of altered cell deformability and aggregability, but they are lacking in the routine clinical tests. In order to measure single RBC volume and surface area, two flow regimes were considered: i) the unbounded flow regime, such as in the case of a 50 μm capillary, where RBCs assume the biconcave disk shape (also found when the cell is at rest); ii) the confined flow regime, such as in the case of capillary of diameter up to 10 μm, where RBCs deform their selves taking a parachute shape. Concerning the unbounded flow condition, the experiments were carried out in a 50 μm capillary. In these conditions, a RBC takes its biconcave disc shape and its contour is discretized by image analysis to measure surface area and volume.

In the confined flow, as happens in a 10 μm capillary, RBC volume and surface area is evaluated by regarding the cell as an axisymmetric solid of revolution around the x axis. On the basis of comparison with Coulter cell analyzer data, we found that high-speed imaging of 10 μm capillary flow provides a reliable way of measuring RBC size parameters (see Table I).

**Table I:** Average values of RBC volume from different methods for 5 healthy donors.

| RBC volume, fL | Average values on 5 donors |
|---|---|
| 50 μm capillary | 71.8 ± 14.2 |
| 10 μm capillary | 85.7 ± 6.37 |
| Coulter counter blood test | 90.32 |

In particular, measurements on RBC surface area, lacking in routine clinical tests, are also obtained (Table II). Unlike impedance measurements, this technique is well suited for monitoring and measuring individual RBC geometrical parameters, such as volume and surface area at a single cell level. It does not require suspending cells in electrolyte solutions and, being a noninvasive technique, could be used to analyze images of flowing RBCs from *in vivo* experiments as well.

**Table II:** Average values of RBC surface area from different methods for 5 healthy donors.

| RBC surface area, $\mu m^2$ | Average values on 5 donors |
|---|---|
| 50 μm capillary | 139 ± 22.5 |
| 10 μm capillary | 120.65 ± 9 |

### 3.5 RBC clustering mechanism

The comprehension of the single cell behavior leaded to the analysis of the RBC flow-induced clustering (Tomaiuolo et al., 2012a). Cluster size and velocity is investigated as a function of the applied pressure drop, including the effect of polydispersity. The two key experimental parameters in this work are the hematocrit, here fixed at 10%, and the imposed pressure drop ΔP across the glass capillary of length of about 2 mm and inner diameter 10 μm.

In Figure 7 cluster length L is plotted as a function of ΔP for different number $N_{RBC}$ of RBCs per cluster, the imposed ΔP being in the physiological range in microcirculation (Cortinovis et al., 2006).

L increases with $N_{RBC}$ and ΔP up to a plateau level, suggesting the presence of a critical length, at about 50 mmHg (the corresponding cell velocity being ~ 1.5 cm/s), above which L stay constant. The analysis of cell distance d within a cluster provides support to the fact that the main variable affecting intercellular separation and RBC deformation is ΔP, which drives cluster dimension to a plateau, whose size is dependent on $N_{RBC}$.

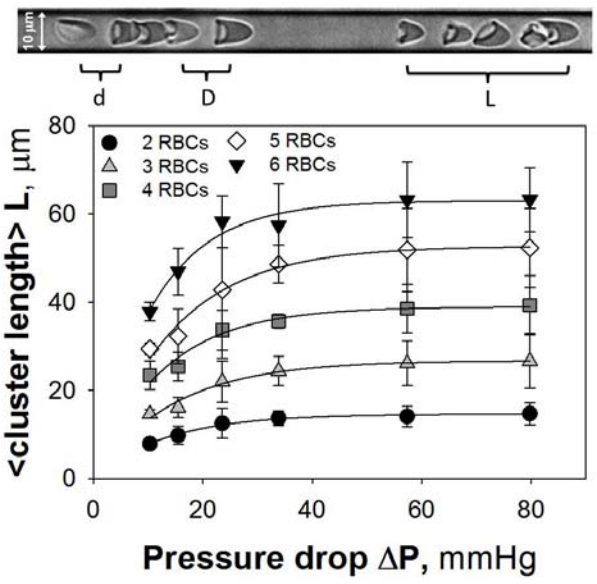


**Figure 7:** RBC cluster parameters (up) and clusters length vs ΔP for different numbers of RBCs (down).

The presence of a limiting cluster length suggests that the forces keeping the cells together in a cluster are of hydrodynamic nature.

Moreover, measurements of the velocity of RBC within a cluster revealed that there is no significant dependence of RBC velocity on cluster size, being the difference between cluster and isolated RBC velocity within 1%.

## Conclusions

This work concerns a systematic investigation of RBC deformation and clustering in artificial microcapillaries with diameter comparable to cell size and in PDMS-based microfluidic devices. The observed RBC parachute shapes and velocities are similar to the ones found *in vivo*, thus showing that this system is indeed a relevant experimental model to study cell microconfined flow behavior.

One of the main results of this work is the development of a novel methodology to estimate cell membrane viscoelastic properties, such as elastic modulus, surface viscosity and relaxation time constant. RBC volume and surface area has been also evaluated, the latter being related to some cardiovascular and thrombotic disorders. Possible applications include the analysis of RBC deformability in pathological situations, for which reliable quantitative methods are still lacking, and the evaluation of the effects of drugs on cell deformability in microcirculation. Furthermore, the data presented in this paper could be used to test recent theoretical and simulation model which predict RBCs behavior under flow in cylindrical microcapillaries, a subject of growing scientific interest (Fedosov et al., 2014a; Fedosov et al., 2014b; Fry et al., 2013).

## References

Abkarian, M., et al., 2008. Cellular-scale hydrodynamics. Biomed Mater. 3**,** 034011.

Barabino, G. A., et al., 2010. Sickle Cell Biomechanics. Annual Review of Biomedical Engineering, Vol 12. 12**,** 345-367.

Bessis, M., et al., 1980. Automated ektacytometry: a new method of measuring red cell deformability and red cell indices. Blood Cells. 6**,** 315-

327.

Buys, A. V., et al., 2013. Changes in red blood cell membrane structure in type 2 diabetes: a scanning electron and atomic force microscopy study. Cardiovascular Diabetology. 12.

Cecchin, E., et al., 1987. Rheological abnormalities of erythrocyte deformability and increased glycosylation of hemoglobin in the nephrotic syndrome. American Journal of Nephrology. 7**,** 18-21.

Cortinovis, A., et al., 2006. Capillary blood viscosity in microcirculation. Clin Hemorheol Microcirc. 35**,** 183-92.

Da Costa, L., et al., 2013. Hereditary spherocytosis, elliptocytosis, and other red cell membrane disorders. Blood Reviews. 27**,** 167-178.

Engstrom, K. G., Meiselman, H. J., 1995. Analysis of red blood cell membrane area and volume regulation using micropipette aspiration and perfusion. Biorheology. 32**,** 115-116.

Evans, E., 1973. A new material concept for the red cell membrane. Biophys J. 13**,** 926-40.

Fedosov, D. A., et al., 2014a. Multiscale modeling of blood flow: from single cells to blood rheology. Biomechanics and modeling in mechanobiology. 13**,** 239-258.

Fedosov, D. A., et al., 2014b. Deformation and dynamics of red blood cells in flow through cylindrical microchannels. Soft Matter. 10**,** 4258-67.

Fry, B. C., et al., 2013. Capillary recruitment in a theoretical model for blood flow regulation in heterogeneous microvessel networks. Physiological reports. 1.

Guido, S., Tomaiuolo, G., 2009. Microconfined flow behavior of red blood cells *in vitro*. C. R. Physique. 10**,** 751–763.

Hochmuth, R., et al., 1979. Red cell extensional recovery and the determination of membrane viscosity. Biophys J. 26**,** 101-14.

Hochmuth, R. M., Micropipette aspiration of living cells. J Biomech, United States, 2000, Vol. 33, pp. 15-22.

Hosseini, S. M., Feng, J. J., 2012. How Malaria Parasites Reduce the Deformability of Infected Red Blood Cells. Biophysical Journal. 103**,** 1-10.

Hénon, S., et al., 1999. A new determination of the shear modulus of the human erythrocyte membrane using optical tweezers. Biophys J. 76**,** 1145-51.

Kohno, M., et al., 1997. Improvement of erythrocyte deformability by cholesterol-lowering therapy with pravastatin in hypercholesterolemic patients. Metabolism-Clinical and Experimental. 46**,** 287-291.

McHedlishvili, G., Maeda, N., 2001. Blood flow structure related to red cell flow: determinant of blood fluidity in narrow microvessels. Jpn J Physiol. 51**,** 19-30.

Mills, J., et al., 2007. Effect of plasmodial RESA protein on deformability of human red blood cells harboring Plasmodium falciparum. Proc Natl Acad Sci U S A. 104**,** 9213-7.

Montagnana, M., et al., The role of red blood cell distribution width in cardiovascular and thrombotic disorders. Clinical Chemistry and Laboratory Medicine, 2012, Vol. 50, pp. 635.

Secomb, T., 1987. Flow-dependent rheological properties of blood in capillaries. Microvasc Res. 34**,** 46-58.

Secomb, T. W., et al., 1986. Flow of axisymmetric red blood cells in narrow capillaries. Journal of Fluid Mechanics. 163**,** 405-423.

Shattil, S., et al., 2000. Hematology: Basic Principles and Practice. Churchill Livingstone, Philadelphia.

Shevkoplyas, S., et al., 2003. Prototype of an in vitro model of the microcirculation. Microvasc Res. 65**,** 132-6.

Smith, B., 1985. Abnormal erythrocyte fragmentation and membrane deformability in paroxysmal nocturnal hemoglobinuria. Am J Hematol. 20**,** 337-43.

Tomaiuolo, G., et al., 2011. Microfluidics

analysis of red blood cell membrane viscoelasticity. Lab Chip. 11**,** 449-54.

Tomaiuolo, G., Guido, S., 2011. Start-up shape dynamics of red blood cells in microcapillary flow. Microvasc Res. 82**,** 35-41.

Tomaiuolo, G., et al., 2012a. Red blood cell clustering in Poiseuille microcapillary flow. Physics of Fluids. 24**,** 051903-8.

Tomaiuolo, G., et al., 2012b. Comparison of two flow-based imaging methods to measure individual red blood cell area and volume. Cytom Part A. 81.

Tomaiuolo, G., et al., 2009. Red blood cell deformability in microconfined shear flow. Soft Matter. 5**,** 3736-3740.

Tsukada, K., et al., 2001. Direct measurement of erythrocyte deformability in diabetes mellitus with a transparent microchannel capillary model and high-speed video camera system. Microvasc Res. 61**,** 231-9.

Wang, C., Popel, A., 1993. Effect of red blood cell shape on oxygen transport in capillaries. Math Biosci. 116**,** 89-110.

Waugh, R. E., Evans, E. A., 1979. Thermoelasticity of red blood cell membranes. Biophysical Journal. 26**,** 115-131.

Whitesides, G. M., 2006. The origins and the future of microfluidics. Nature. 442.

Zhang, H., Liu, K. K., 2008. Optical tweezers for single cells. J R Soc Interface. 5**,** 671-90.